

## THE PROGENITOR OF GW 150914

S. E. WOOSLEY<sup>1</sup>*Draft version October 8, 2018*

## ABSTRACT

The spectacular detection of gravitational waves (GWs) from GW 150914 and its reported association with a gamma-ray burst (GRB) offer new insights into the evolution of massive stars. Here it is shown that no single star of any mass and credible metallicity is likely to produce the observed GW signal. Stars with helium cores in the mass range 35 to 133  $M_{\odot}$  encounter the pair instability and either explode or pulse until the core mass is less than 40  $M_{\odot}$ , smaller than the combined mass of the observed black holes. The rotation of more massive helium cores is either braked by interaction with a slowly rotating hydrogen envelope, if one is present, or by mass loss, if one is not. The very short interval between the GW signal and the observed onset of the putative GRB in GW 150914 is also too short to have come from a single star. A more probable model for making the gravitational radiation is the delayed merger of two black holes made by 70 and 90  $M_{\odot}$  stars in a binary system. The more massive component was a pulsational-pair instability supernova before making the first black hole.

*Subject headings:* supernovae: general; black holes; gravitational radiation

## 1. INTRODUCTION

The detection by Abbott et al. (2016) of gravitational radiation from a pair of merging massive black holes,  $36^{+5}_{-4}$  and  $29^{+4}_{-4}$   $M_{\odot}$ , has ushered in a new era of multi-messenger astronomy. Motivated largely by the reported coincident gamma-ray burst (Connaughton et al. 2016), Loeb (2016) suggested that a single star model might have produced GW 150914. He assumes the precursor to the collapse contains a rapidly rotating helium core of at least 65  $M_{\odot}$  (the sum of the masses of the observed black hole pair) that has formed as the result of a prior merger of stars in a binary system. The core rotates so rapidly that it fissions into two black holes during its collapse. The two black holes recombine emitting the observed GW.

Well before the GW detection, Fryer et al. (2001) calculated an alternative, single star model for a burst of gravitational radiation accompanied by a GRB, but invoked a much more massive star, 300  $M_{\odot}$ , with a 180  $M_{\odot}$  helium core. Their 2D calculation was unable to directly demonstrate the fission of the collapsing core, but rotational energy and angular momentum considerations suggested that as a possible outcome.

Here it is shown that both of these scenarios are unlikely to produce the observed GW event. Helium cores anywhere near 65  $M_{\odot}$ , and up to 133  $M_{\odot}$ , encounter the pair instability, and either pulse violently and lose mass (Woosley et al. 2007; Woosley & Heger 2015), or explode (Heger & Woosley 2002). They do not make black holes having a total mass greater than about 40  $M_{\odot}$ . For helium cores above 133  $M_{\odot}$  black hole production is indeed likely, but when reasonable estimates of magnetic torques and mass loss are included (Heger et al. 2005), the collapsing core contains too little angular momentum to bifurcate.

Any stellar channel for producing GW 150914 must therefore involve binary evolution. Here it is shown that the observationally inferred masses for the merging black

holes,  $36^{+5}_{-4}$  and  $29^{+4}_{-4}$   $M_{\odot}$ , could result from the evolution of stars of non-rotating stars of 70 and 90  $M_{\odot}$  with metallicity less than about 10% solar. If rotation is included, the inferred masses are closer to 60 and 70  $M_{\odot}$ . Interestingly, the heavier star of each pair not only produces a black hole near 36  $M_{\odot}$ , but also makes a pulsational-pair instability supernova (PPISN) that ejects any low density envelope shortly before collapse, but does not unbind the system.

## 2. THE FAILURE OF SINGLE STAR MODELS FOR GW 150914

Since the hydrogen envelope will not participate in any prompt collapse, a minimum helium core mass equal to the sum of the observed black hole masses is required in any single star model, i.e.,  $M_{\alpha} > 65$ . Since it is unlikely that the entire helium core collapsed during the less than 1 second duration of the GW signal, this is a lower bound, possibly an extreme one (Woosley et al. 1986). Such a large helium core could be the consequence of a single star of mass over 150  $M_{\odot}$ , the merger of two lighter stars, or the chemically homogeneous evolution of a star as small as 65  $M_{\odot}$ .

To guide the discussion, a set of models (Table 1) was calculated using the KEPLER code (Weaver, Zimmerman, & Woosley 1978; Woosley et al. 2002, e.g.). The models had in common a low metallicity, 10% that of the sun, chiefly employed to keep the mass loss rate low. Most of the models that included rotation also included magnetic torques (Heger et al. 2005) that acted to brake the rotation of the helium core at late times and enforce rigid rotation. Modern, but uncertain mass loss rates were included (Nieuwenhuijzen & de Jager 1990). For hydrogen burning stars with surface hydrogen mass fractions more than 0.4, a metallicity scaling of  $Z^{0.5}$  was employed. For chemically homogeneous models with lower surface hydrogen mass fractions, the Wolf-Rayet mass loss rate of Braun (1997) was employed as modified for clumping by Woosley & Heger (2006) with a metallicity scaling of  $Z^{0.86}$  (Vink & de Koter 2005). All stars considered would have lost their hydrogen envelopes and most of

<sup>1</sup> Department of Astronomy and Astrophysics, University of California, Santa Cruz, CA 95064; woosley@ucolick.org

TABLE 1. LOW METALLICITY MODELS

Models	Mass Loss	M <sub>ZAMS</sub>   M <sub>preSN</sub>   M <sub>remnant</sub>			M <sub>α</sub>   M <sub>CO</sub>   M <sub>Si</sub>   M <sub>Fe</sub>		Pulse Activity				
		[M <sub>⊙</sub> ]			[M <sub>⊙</sub> ]		t <sub>p</sub> [10 <sup>6</sup> s]	E <sub>p</sub> [10 <sup>50</sup> ergs]			
no rotation	T70A	1	70	55.5	55.5	30.1	26.4	7.87	2.58	0.059	-
	T70B	0	70	70.0	70	31.6	28.0	8.41	2.57	0.055	-
	T90A	1	90	66.5	35.9	39.7	35.4	9.54	2.57	1.1	5.6
	T90B	0	90	90.0	37.1	40.9	36.8	8.35	2.86	1.9	4.9
	T150	1	150	96.0	0	65.1	55.2	- PSN	-	-	77
rotating	R60	1/2	60	52.4	52.3	30.9	26.6	8.18	2.64	0.047	-
	R70	1	70	56.9	34.5	37.4	32.9	10.3	2.72	0.32	4.5
	R110	1/2	110	102	0	66.7	60.3	- PSN	-	-	62
	R150A	0	150	150	150	150	-	- BH	-	-	-
	R150B	1	150	28.4	28.4	28.4	24.3	6.55	2.58	-	-
	R150C	1	150	122	0	122	118	- PSN	-	-	768
	R300A	0	300	300	300	161	-	- BH	-	-	-
	R300B	0	300	300	300	180	-	- BH	-	-	-
	R300C	1	300	143	143	143	-	- BH	-	-	-

their helium cores had they been of solar metallicity.

Models starting with “T” in Table 1 were not rotating; those starting with “R” included rotation. One non-rotating model, T150, had a final helium core mass of 65 M<sub>⊙</sub> and illustrates that helium cores of this mass explode as ordinary PISN. They do not make black holes. Including rotation is not likely to alter this outcome Chatzopoulos et al. (2013); Chen (2015), though it does reduce the main sequence mass required to produce the helium core (Model R110).

Two other sets of models were calculated that included rotation. Models R300 were based on the evolution of single stars of 10% solar metallicity with initial masses of 300 M<sub>⊙</sub>. Each had a total initial angular momentum of  $1.5 \times 10^{54}$  erg s and an equatorial rotational speed of 180 km s<sup>-1</sup>. Model R300A did not include mass loss or magnetic torques, and is thus very similar to the case studied by Fryer et al. (2001). Model R300B included magnetic torques but not mass loss; R300C included both mass loss and magnetic torques. Models R150 are discussed later.

Fig. 1 shows the distribution of specific angular momentum,  $j$ , in the three 300 M<sub>⊙</sub> models at the point of pair instability. The central temperature in each exceeded  $3 \times 10^9$  K and no further redistribution of  $j$  will occur. The helium core here is about 10% less than that of Fryer et al. (2001) because convective dredge up was less efficient in the new calculation, but the angular momentum distribution is quite similar (compare the black line in Fig. 1 with their Fig. 2). The total angular momentum of the helium core is  $2.36 \times 10^{53}$  erg s. As Fryer et al. (2001) noted, this is sufficient angular momentum to form a disk, and perhaps even to bifurcate and emit copious gravitational radiation in its final stage of collapse.

Unfortunately, as Fig. 1 also shows, the inclusion of magnetic torques and mass loss greatly alters the outcome. The helium core still exceeds the critical mass, 133 M<sub>⊙</sub>, for producing a black hole, but its angular momentum is greatly reduced by interacting with the slowly rotating hydrogen envelope. The angular momentum in the helium core of R300B at collapse is reduced by a factor of 10 to  $2.48 \times 10^{52}$  erg s, and inadequate even to make a disk anywhere except perhaps in the outer-

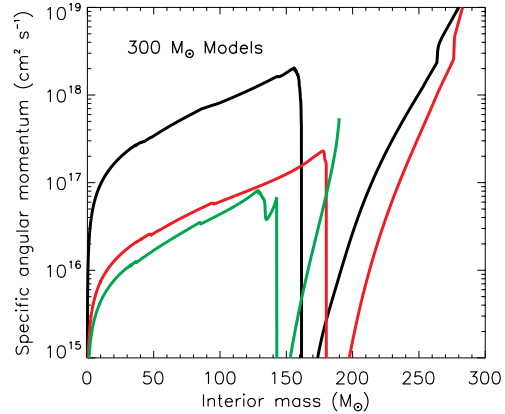


FIG. 1.— Final angular momentum distribution at collapse of a 300 M<sub>⊙</sub> model evolved with no mass loss or magnetic torques (black line); magnetic torques, but no mass loss (red line); and mass loss plus magnetic torques (green line). The edge of the helium core is apparent where the angular momentum sharply drops and then rises again. Both models that include magnetic torques have too little angular momentum for the core to bifurcate or form a disk during its collapse to a black hole. The Kerr parameter is of order unity for the black curve, but everywhere less than 0.1 for the green and red curves. The helium cores of all three models are sufficiently massive to collapse directly to black holes.

most core. Model R300C, with torques and mass loss, is worse, with a total angular momentum in the helium core of only  $8.74 \times 10^{51}$  erg s and insufficient angular momentum to make a disk anywhere in the core. Models R300B and 300C, which are more realistic than R300A, will not make the observed GW signal.

One might object that the mass loss rates and especially the prescription for magnetic torques are uncertain. This is true, but the magnetic torques used here give approximately the right rotation rates for newly born pulsars (Heger et al. 2005) and, if anything, might need to be larger. Neglecting them leads to most massive stars dying with sufficient angular momentum to make a millisecond magnetar. The fact that gamma-ray bursts are so rare, is thus an argument that magnetic torques of

a magnitude not too different from that assumed here must play a role in the evolution of massive stars.

One way to give the core additional angular momentum might be to avoid the production of any red supergiant phase and invoke chemically homogeneous evolution (CHE) on the main sequence (Woosley & Heger 2006; Yoon et al. 2012; Chatzopoulos & Wheeler 2012; Köhler et al. 2015). This is the tack taken by those attempting to explain the rapid rotation of gamma-ray burst progenitors, and would presumably correspond to a rare event limited to stars of unusually rapid rotation. To test this possibility, three more models were calculated with a lower mass, but greater specific angular momentum to insure CHE. Models R150, with mass  $150 M_{\odot}$ , had an initial total angular momentum of  $1 \times 10^{54}$  erg s and rotated at  $325 \text{ km s}^{-1}$  on the main sequence. Each experienced CHE and included magnetic torques. Model R150A had no mass loss though, while Models R150B and R150C had a mass loss rate equal to the full value or 10% of the full value expected for a star with metallicity 10% that of the sun.

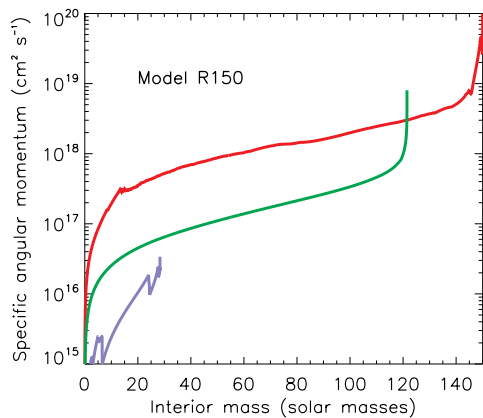


FIG. 2.— Final angular momentum distribution in a  $150 M_{\odot}$  model evolved including sufficient angular momentum that it experiences complete mixing on the main sequence. Model R150A (top red line) had no mass loss. Models R150B (bottom blue line) and R150C (middle green line) included 100% and 10% respectively of the mass loss expected for a star with 10% solar metallicity.

The results for Model R150A are encouraging. By the time the central density reached  $10^{11} \text{ g cm}^{-3}$  when neutrino trapping might occur, the ratio of rotational energy to gravitational potential energy,  $T/W$ , exceeded 20% in the inner  $10 M_{\odot}$ , and was greater than 12% everywhere in the star. The Kerr parameter was substantially greater than unity throughout the entire core, guaranteeing that angular momentum will be lost, either through a disk or fission and gravitational radiation, before even a maximally rotating black hole forms. The subsequent evolution would probably be similar to that of the  $180 M_{\odot}$  core of Fryer et al. (2001, Compare with their Fig. 3) in 2D and, possibly, to the calculations of Reisswig et al. (2013) in 3D.

Unfortunately, this is not a credible model since mass loss must be included. If the mass loss appropriate to a 10% solar metallicity star is used, the star nearly evaporates (Fig. 2). Not only is the final mass too small to

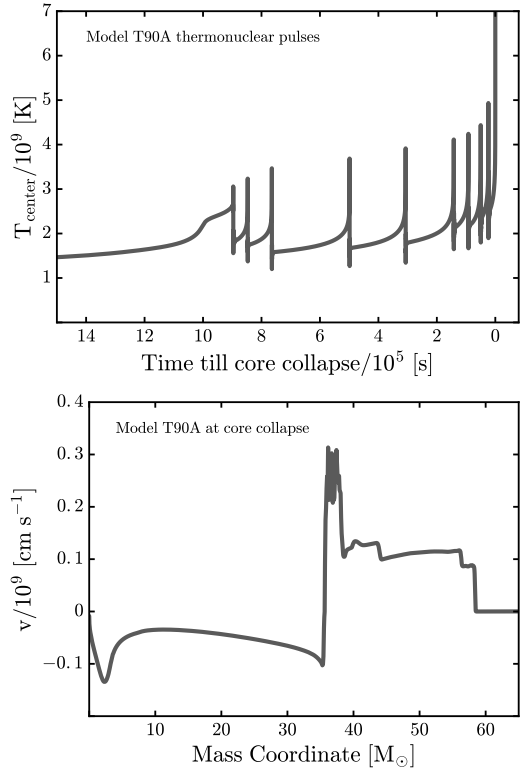


FIG. 3.— Pulse history and collapse velocity for Model T90A.

make the pair of black holes, the amount of residual angular momentum is trivial.

Mass loss rates are uncertain and perhaps the metallicity was even lower than  $0.1 Z_{\odot}$ , so model R130C used ten times less mass loss. This would make the model comparable to those studied by Köhler et al. (2015) for massive stars in the galaxy I Zwicky 18 with metallicity  $10^{-1.7}$  that of the sun. Indeed, at hydrogen depletion, the remaining mass for Model R150C here,  $139 M_{\odot}$ , is close to what they calculated for a star of similar rotation rate,  $136 M_{\odot}$ . Much more mass loss occurs during helium burning though, and the star ends up with a final mass of  $122 M_{\odot}$ . This is too small to produce a black hole, but that deficiency might be alleviated by taking a more massive main sequence star. More problematic is the low angular momentum in the star at death,  $5.0 \times 10^{52}$  erg s. While adequate to produce a disk in the outer core if a black hole formed, the angular momentum in the inner core is too little to cause fission.

Thus single star models that include magnetic torques and mass loss fail to produce a system that could explain GW 150914. If an envelope is present the core is braked too much by the interaction. If the envelope is absent, mass loss from the core has the same consequence.

### 3. A BINARY MODEL FOR GW 150914

Alternatively, as suggested many times before the event was observed, (Belczynski et al. 2010, 2016a; Marchant et al. 2016; Mandel & de Mink 2016, e.g.), the two black holes could be made separately in a binary system and brought together by a combination of common envelope evolution and gravitational radiation.

To provide some detail to these suggestions, which did

not include the evolution of the stars to their collapse, several other models were calculated (Table 1). The main sequence masses here were chosen to produce helium cores in the resulting presupernova star near 29 (Models T70 and R60) and 36  $M_{\odot}$  (Models T90 and R70). Models T70 and T90 did not include rotation. Models R60, R70, and R110 had an equatorial rotation speed on the main sequence of 160 - 180  $\text{km s}^{-1}$  corresponding to a ratio of centrifugal force to gravity of approximately 15%. These models did not experience chemically homogeneous evolution, and their helium core masses were substantially less than their final masses. All models ended their (single star) lives as red supergiants. Since mass loss is uncertain, some models were run both with and without mass loss (A and B). The results show that the dependency of final helium core mass on the mass loss rate is weak, so long as the entire envelope is not lost. For those models that experienced the pulsational pair instability, the number of pulses and total energy in pulses are given. No pulse energies are given for Models T70 and R60 because they were very weak and the envelope was not ejected.

### 3.1. The Components

Model T90A, which is exemplary of stars that make a 36  $M_{\odot}$  black hole, encountered the pulsational-pair instability at carbon depletion. This resulted in nine strong thermonuclear pulses occurring during the last  $10^6$  s of the star's life (Fig. 3). Following each flash, the core expanded, emitted a shock wave into the hydrogen envelope, then relaxed, and encountered the pair instability again. These flashes derived their energy from explosive oxygen and silicon burning in the inner 5  $M_{\odot}$  of the core. Eventually the pulses ejected the envelope leaving most of the helium core intact and stable against further pulsation. The residual core evolved to produce an iron core of 2.57  $M_{\odot}$  (Model T90A) or 2.86  $M_{\odot}$  (Model T90B). While the subsequent evolution of the iron core was not followed here, given its large size and the shallow density gradient outside, it is unlikely to explode by neutrino transport (Ertl et al. 2016, e.g.). Lacking rotation, the protoneutron star accretes for perhaps a second and becomes a black hole. The remaining core of helium and heavy elements quickly accretes into the hole. The baryonic mass of the collapsed remnant is 35.9  $M_{\odot}$  for Model T90A and 37.1  $M_{\odot}$  for Model T90B, though a few tenths of a solar mass should be subtracted because of the neutrino losses during the protoneutron star phase (O'Connor & Ott 2011).

The velocity structure at the time when the iron core of T90A collapses is shown in Fig. 3. Despite the collapse of the core to a black hole, the shock waves from the pulses propagate into the hydrogen envelope long after the core has collapsed, and ultimately eject it with a kinetic energy  $\sim 5 \times 10^{50}$  erg (Table 1). This leads to a rather ordinary Type IIp supernova lasting about 200 days with a luminosity on the plateau of about  $2 \times 10^{42}$  erg s $^{-1}$ .

Adding rotation to the model does not change the qualitative result, though it does alter the main sequence mass required to produce the given black hole mass. Model R70 produces a helium core of 37.4  $M_{\odot}$  that also encounters the pulsational-pair instability and ejects its hydrogen envelope and a portion of the core. In the end,

a remnant with baryonic mass 34.5  $M_{\odot}$  is left and the hydrogen envelope is ejected producing a Type IIp supernova. Following the transport of angular momentum that happens during carbon, neon, and oxygen burning and in the pulses, including magnetic torques, gives an angular momentum in the collapsing core of less than  $10^{16} \text{ cm}^2 \text{ s}^{-1}$  in the inner 20  $M_{\odot}$ . Even at the edge of the helium core,  $j$  is only  $4 \times 10^{16} \text{ cm}^2 \text{ s}^{-1}$ . The core collapses to a black hole and does not form a disk.

The evolution of the lighter component, as exemplified by Model T70A, is similar, but less explosive. This star too encounters a weak pulsational-pair instability in its oxygen shell during the waning hour of its life, but the pulses are too weak to eject even the loosely bound envelope. The 30.1  $M_{\odot}$  helium core collapses directly to a black hole leaving most of its envelope still bound. In a single star system without rotation, the envelope too would accrete over a period of days, finally producing a black hole of 55.5  $M_{\odot}$  (Table 1).

### 3.2. Binary Evolution

Now consider these two stars interacting in a binary system with initial separation of order several AU. On the main sequence, the stellar radii are sufficiently small,  $8.4 \times 10^{11}$  cm and  $9.8 \times 10^{11}$  cm for Models T70A and T90A, that the stars evolve individually. When T90A burns helium however, it fills its Roche lobe and starts to spill over onto Model T70A. In solitude, T90A develops a radius of 0.5, 1.0, 3.0, and 6.0 AU when its central helium mass fraction is 0.978, 0.923, 0.5, and 0.01 respectively. It finally reaches a radius of 11 AU after helium depletion when the star has only a few thousand years to live.

The subsequent evolution, especially through one or more stages of common envelope, is very uncertain (Ivanova et al. 2013), but might resemble the system described by Belczynski et al. (2016b). Their initial binary contains two stars of 96.2 and 60.2  $M_{\odot}$  with metallicity 3%  $Z_{\odot}$  (their progenitors were born in the early universe) separated by 11.4 AU. A stage of Roche lobe overflow strips the primary of its envelope leaving a helium core of 39  $M_{\odot}$ , similar to models T90AB and R70 here. Half of the envelope is lost from the system. That helium core collapses to a 35.1  $M_{\odot}$  black hole following a loss of 10% of the mass to neutrino emission. Later evolution of the secondary leads to a common envelope that brings the black hole and the helium core of the secondary into close proximity after the envelope is ejected. The core of the secondary collapses to a second black hole of 30.8  $M_{\odot}$  in a nearly circular orbit with separation 0.22 AU. The black holes merge 10.3 Gy later.

Several differences exist with the models in this paper. First, the models here have higher metallicity and may lose appreciable mass besides mass exchange. Given the key role of the helium cores, the envelope masses may not be so critical, but they do affect the parameters of the later common envelope evolution. The slow expansion of Model T90 to supergiant proportions, likely a consequence of the way semiconvection is treated in the code, may require a closer initial orbital separation than assumed by Belczynski et al. (2016b) to transfer its entire envelope to the secondary. This too may not matter much because Model T90A becomes a supernova before making a black hole and ejects any remaining envelope. The orbital separation when the first black hole forms

would be affected though.

Both black holes are formed here by the collapse of iron cores near  $2.6 M_{\odot}$ . There will of necessity be a brief phase of proto-neutron star formation and neutrino emission before a black hole of about  $3 M_{\odot}$  forms. The neutrino losses from that stage are likely to be only a few tenths of a solar mass (O'Connor & Ott 2011), and the efficiency for neutrino emission declines greatly after the event horizon forms (Woosley et al. 1986). The mass decrement may thus not be as large as the 10% assumed by Belczynski et al. (2016b). Black hole kicks may also be smaller.

A common envelope phase is necessary to bring the black hole and core of the secondary close enough to merge in a reasonable time. The expansion history of T70A is thus important. Assuming its core structure is not greatly altered by the mass accreted during the first Roche lobe overflow, T70A ignites helium burning 55,000 years after birth of the first black hole (death of T90A) and expands to 1 AU 110,000 years later, when the helium is half burned. At helium depletion, 210,000 years after that, the radius is 6.5 AU. Sometime in between, a common envelope presumably forms, but how close will that envelope bring the black hole to the helium core before it too collapses? Estimates typically employ a comparison of envelope binding energies and core separations plus some efficiency factor  $\alpha$  (Ivanova et al. 2013). A final separation of less than 0.2 AU, like Belczynski et al. (2016b) require and obtain, implies a gravitational potential for two  $\sim 30 M_{\odot}$  masses of about  $8 \times 10^{49}$  erg. The *net* binding energy outside 0.2 AU in the T70A pre-supernova star is only  $3 \times 10^{48}$  erg, but additional energy is expended ejecting matter pushed up from beneath during the common envelope phase and providing it with ejection speed. The total net binding energy of the matter outside the hydrogen helium discontinuity in Model T70A at  $31.0 M_{\odot}$  is indeed large,  $2.3 \times 10^{50}$  erg.

#### 4. CONCLUSIONS

The characteristics of GW 150914 are unlikely to be explained by any single star model. The model before the event (Fryer et al. 2001) errs in neglecting the magnetic coupling between the rapidly rotating helium core and the nearly stationary hydrogen envelope and in neglecting mass loss. The model after the event (Loeb 2016) errs in invoking an extremely rapidly rotating helium core for which there is no clear path in current stellar evolution. An alternative model based on chemically homogeneous evolution shows promise until mass loss is included. This model might work if there were no mass loss and could potentially occur in extremely low metallicity stars -  $\sim 10^{-3} Z_{\odot}$ , but not in stars expected in the galaxy where the merger was detected.

Similar considerations apply to models based on merger of massive stars prior the black hole formation. Though, in principle, a rapidly rotating helium core could be formed, so long as an envelope remained, magnetic torques would rapidly brake its rotation. If the envelope were ejected, mass loss during helium burning would brake the core.

In any case, one of the key motivations for single star

models, namely explaining the putative GRB temporally coincident with GW 150914, is not satisfied. The Fermi/GBM team reported a possible transient about 0.4 s after the reported LIGO burst trigger time, and lasting for about one second (Blackburn et al. 2015; Connaughton et al. 2016), though that detection is head of controversial. Studies by Zhang et al. (2004) have shown that the the GRB producing jet travels significantly slower than the speed of light while inside the star that makes it. The jet has far less mass than the star it working surface, where the jet pushes aside stellar matter, moves at only about  $c/3$  and thus takes about 10 s to exit a star with radius  $8 \times 10^{10}$  cm in the Zhang study. The most optimistic model here, R150A has a radius of  $6 \times 10^{10}$  cm when it dies and a much greater density than the model studied by Zhang et al. The observed GRB here was a weak short one. Thus it is quite unlikely that the jet would reach the surface in less than 10 s. The GW signal, on the other hand, reaches the surface in 2 s and remains forever 8 s ahead of the GRB. That this exceeds the observed delay by a factor of 10 is a severe problem that should be kept in mind for future studies of coincident GRBs and GW signals. A repeat of Zhang's calculation using, e.g., model R150A, would be useful to clarify the expected delay. If the star still had an envelope, there would have been no GRB. Alternatively, it might be possible to make a prompt GRB by merging two black holes if one or both have a fossil disk (Perna et al. 2016).

Indeed, the most likely model for GW 150914 is the one suggested beforehand. Two massive stars make two black holes that, under the influence of first, a common envelope, and later, gravitational radiation, come together long after their creation. The evolution of rotating and non-rotating stars that might produce black holes with the measured masses were considered here and found to hover on the edge of the pair instability. The more massive primary especially is capable of ejecting its hydrogen envelope owing to thermonuclear pulses without binary mass transfer, though that does not preclude the transfer happening. Both stars produce iron cores in hydrostatic equilibrium with masses of about  $2.6 M_{\odot}$  that collapse first to proto-neutron stars, and emit a few tenths of a solar mass in neutrinos before becoming black holes into which the rest of the core accretes. Given the small mass lost, large kicks seem unlikely.

In the future it is hoped that realistic simulations of presupernova evolution in this mass range can be coupled to models for common envelope evolution to better describe the progenitor of this fascinating event.

#### 5. ACKNOWLEDGEMENTS

This research has been partially supported by NASA (NNX14AH34G). The author appreciates the long term assistance of Alex Heger with the development of the KEPLER code and helpful conversations with Chris Belczynski about the nature of common envelope evolution.

## REFERENCES

- Abbott, B. P., et al. 2016, *Phys. Rev. Lett*, 116, 061102
- Belczynski, K., Dominik, M., Bulik, T., et al. 2010, *ApJ*, 715, L138
- Belczynski, K., Repetto, S., Holz, D. E., et al. 2016, *ApJ*, 819, 108
- Belczynski, K., Holz, D. E., Bulik, T., & O’Shaughnessy, R. 2016, arXiv:1602.04531
- Blackburn, L., Briggs, M. S., Burns, E., et al. 2015, *GRB Coordinates Network*, 18339
- Braun, H. 1997, PhD thesis, Ludwig-Maximilians Universität München
- Chatzopoulos, E., & Wheeler, J. C. 2012, *ApJ*, 748, 42
- Chatzopoulos, E., Wheeler, J. C., & Couch, S. M. 2013, *ApJ*, 776, 129
- Chen, K.-J. 2015, *Modern Physics Letters A*, 30, 1530002
- Connaughton, V., et al. 2016, arXiv:1602.03920
- Ertl, T., Janka, H.-T., Woosley, S. E., Sukhbold, T., & Ugliano, M. 2016, *ApJ*, 818, 124
- Fryer, C. L., Woosley, S. E., & Heger, A. 2001, *ApJ*, 550, 372
- Heger, A., & Woosley, S. E. 2002, *ApJ*, 567, 532
- Heger, A., Woosley, S. E., & Spruit, H. C. 2005, *ApJ*, 626, 350
- Ivanova, N., Justham, S., Chen, X., et al. 2013, *A&A Rev.*, 21, 59
- Köhler, K., Langer, N., de Koter, A., et al. 2015, *A&A*, 573, A71
- Loeb, A. 2106, *ApJ* in press, arXiv:1602.04735.
- Mandel, I., & de Mink, S. E. 2016, *MNRAS*, 458, 2634
- Marchant, P., Langer, N., Podsiadlowski, P., Tauris, T. M., & Moriya, T. J. 2016, *A&A*, 588, A50
- Nieuwenhuijzen, H., & de Jager, C. 1990, *A&A*, 231, 134
- O’Connor, E., & Ott, C. D. 2011, *ApJ*, 730, 70
- Perna, R., Lazzati, D., & Giacomazzo, B. 2016, *ArXiv e-prints*, arXiv:1602.05140
- Reisswig, C., Ott, C. D., Abdikamalov, E., et al. 2013, *Physical Review Letters*, 111, 151101
- Savchenko, V., Ferrigno, C., Mereghetti, S., Natalucci, L., et al, 2016, *ApJ*, 820, L36
- Szécsi, D., Langer, N., Yoon, S.-C., et al. 2015, *A&A*, 581, A15
- Vink, J. S., & de Koter, A. 2005, *A&A*, 442, 587
- Weaver, T. A., Zimmerman, G. B., & Woosley 1978, *ApJ*, 225, 1021
- Woosley, S. E., Wilson, J. R., & Mayle, R. 1986, *ApJ*, 302, 19
- Woosley, S. E., Heger, A., & Weaver, T. A. 2002, *Reviews of Modern Physics*, 74, 1015
- Woosley, S. E., & Heger, A. 2006, *ApJ*, 637, 914
- Woosley, S. E., Blinnikov, S., & Heger, A. 2007, *Nature*, 450, 390
- Woosley, S. E., & Heger, A. 2015, *Astrophysics and Space Science Library*, 412, 199
- Yoon, S.-C., Dierks, A., & Langer, N. 2012, *A&A*, 542, A113
- Zhang, W., Woosley, S. E., & Heger, A. 2004, *ApJ*, 608, 365